Geology of the Hookers Hot Springs area, Galiuro Mountains, southeastern Arizona

Jon E. Spencer[1], Brad J. Johnson[1] and L Peters[2]

[1]Arizona Geological Survey

[2]New Mexico Geochronology Research Laboratory

Conglomerate exposed near Hooker Hot Spring(Photo by B.J. Johnson)

OPEN-FILE REPORT OFR-15-06

September 2015

Arizona Geological Survey

www.azgs.az.gov | repository.azgs.az.gov

Arizona Geological Survey

M. Lee Allison, State Geologist and Director

Manuscript approved for publication in September 2015
Printed by the Arizona Geological Survey
All rights reserved

For an electronic copy of this publication: www.repository.azgs.az.gov
Printed copies are on sale at the Arizona Experience Store
416 W. Congress, Tucson, AZ 85701 (520.770.3500)

For information on the mission, objectives or geologic products of the Arizona Geological Survey visit www.azgs.az.gov.

This publication was prepared by an agency of the State of Arizona. The State of Arizona, or any agency thereof, or any of their employees, makes no warranty, expressed or implied, or assumes any legal liability or responsibility for the accuracy, completeness, or usefulness of any information, apparatus, product, or process disclosed in this report. Any use of trade, product, or firm names in this publication is for descriptive purposes only and does not imply endorsement by the State of Arizona.

Recommended Citation: Spencer, J.E., Johnson, B.J and Peters, L. , 2015, Geology of the Hookers Hot Springs area, Galiuro Mountains, southeastern Arizona. Arizona Geological Survey Open File Report, OFR-15-06, 21 p, 2 appendices.

Geology of the Hookers Hot Springs area, Galiuro Mountains, southeastern Arizona

Jon E. Spencer and Bradford J. Johnson, Arizona Geological Survey
Lisa Peters, New Mexico Geochronology Research Laboratory

Introduction

Hookers Hot Springs is located approximately 70 km (40 miles) east of Tucson, Arizona, and is within the Hookers Hot Springs 7.5' Quadrangle in the southern Galiuro Mountains. The hot spring itself is on the southwest flank of the wide wash in Hot Springs Canyon, east of the San Pedro River. Water temperature is reported at 52° C. Hookers Hot Springs and surrounding land are part of the Nature Conservancy's Mule Shoe Ranch Preserve. Arizona Geological Survey geologists were granted permission to access the area in 2014. Jon Spencer and Brad Johnson of the Arizona Geological Survey mapped the geology of approximately 18 km^2 (7 mi^2) to identify geologic features that potentially influence groundwater hydrology. Lisa Peters of the New Mexico Geochronology Research Laboratory determined the age of three rock samples. It was hoped that geologic features could be identified that are responsible for the hot water emanating from the spring. Ultimately, this geologic study was intended to provide better understanding of the geothermal resources in the area. Funding for this study was provided by the U.S. Department of Energy under the National Geothermal Data System Supplemental Project, Contract DE-EE0002850 (Love et al., 2014).

Regional geology

Hookers Hot Springs are within the southern Galiuro Mountains, an approximately 100 km long, north-northwest trending mountain range that consists primarily of 20-30 million-year-old volcanic rocks (Dickinson and Shafiqullah, 1989; Dickinson, 1991; Richard et al., 2000). The range itself resembles a typical Basin and Range fault block (horst), with flanking normal faults dipping outward from the range. Many of the bounding normal faults, however, dip gently rather than steeply away from the range (Davis and Hardy, 1981; Dickinson et al., 1987; Goodlin and Mark, 1987; Dickinson, 1991).

Volcanic rocks in the range are older than ~25 Ma, which is too old to be a heat source for thermal springs. There is no known evidence geologically recent magmatic activity that could have provided heat for hot-spring activity, and no young igneous rocks were identified in this study.

Geology of the Hookers Hot Springs area

The Galiuro Mountains bifurcate southward into two narrow ranges separated by an intramontane basin that includes Allen Flat and upper Hot Springs Canyon (Allen Flat basin of Burtell, 1989). The western range includes the Johnny Lyon Hills, while the Winchester Mountains form the eastern range. Hot Springs Canyon drains much of the area in this intramontane basin, and crosses the western side of the Galiuro Mountains to enter the San Pedro River. Hookers Hot Springs is located about a half kilometer upstream from the point where Hot Springs Canyon Wash flows from the intramontane basin to cut across bedrock in the southwestern Galiuro Mountains (Figure 1; Appendix 1). The boundary between these two geographic features is a steeply east-dipping, east-side-down normal fault, located ~600 m downstream from Hookers Hot Springs (Figure 1). The basin sediments incised by upper Hot Springs Canyon and its tributaries consist of poorly to moderately lithified, poorly sorted, sandy pebble and cobble conglomerate with generally crudely defined bedding (map unit Tcg in Figure 1 and Appendix 1). Clasts in the conglomerate were derived primarily from the older volcanic units that were probably eroded from the nearby Winchester Mountains. Beds in the conglomerate are generally gently dipping, but near the basin-bounding normal fault west and south of Hookers Hot Springs, bedding is steeper with an approximately 30° dip to the west-southwest. Beds here projects down-dip into the normal fault with a bedding-fault intersection angle of ~90° (Figure 2B).

North of Hot Springs Wash the steep normal fault dies out into a steeply east-dipping depositional contact. Beds in the basin-filling conglomerate unit dip moderately to steeply eastward near the depositional contact, with bedding dips decreasing up section to the east so that more than ~1 km away beds are gently dipping (Figures 1, 2A). Based on cross section A (Fig. 2A) we estimate that the preserved thickness of the conglomerate unit is ~400 m. The northward transition from a normal fault with adjacent west-dipping beds to a depositional contact with adjacent east-dipping beds is unusual, and we are not aware of a similar structure anywhere in Arizona. Conglomerate beds in northern exposures are folded, reflecting horizontal shortening, whereas to the south, a normal fault offsets conglomerate beds, reflecting horizontal extension.

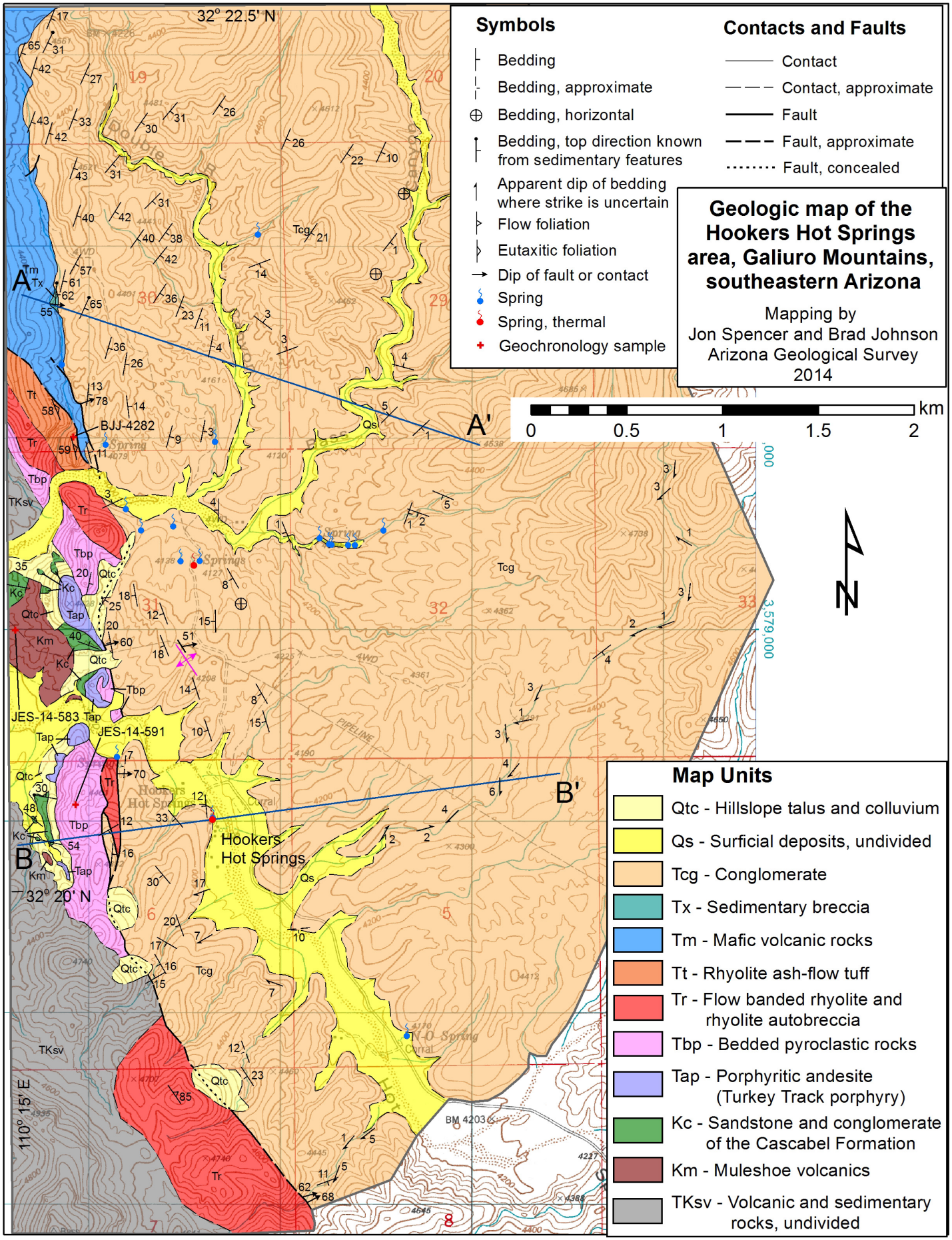

Figure 1. Geologic map of the Hookers Hot Springs area.

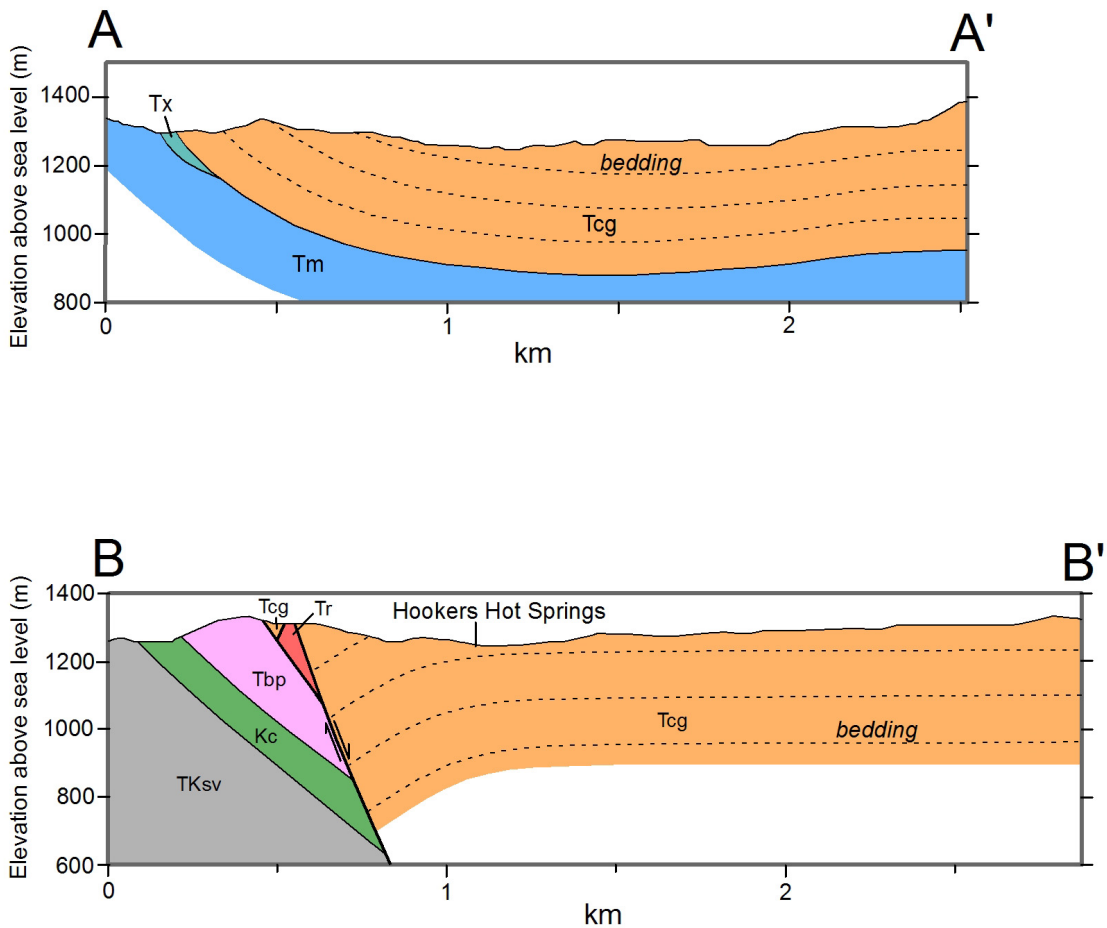

Figure 2. Geologic cross sections of the Hookers Hot Springs area. See Figure 1 for location.

The implication of this structural contrast is that fault blocks on opposite sides of the fault were rotated relative to each other about a pivot point ~1 km north of Hookers Hot Springs, with shortening to the north and extension to the south. The fact that the areal extent of east-tilted beds increases northward is consistent with this interpretation, and suggests that a reverse fault in the subsurface accommodates shortening in basement rocks.

New $^{40}Ar/^{39}Ar$ geochronologic results from three volcanic rock units (Appendix 2) indicate that the volcanic rocks that directly underlie the basin-filling sediments are 27-28 Ma (million years old) and so are too old to be a source of heat for thermal springs. Underlying Mule Shoe volcanics are even older, yielding a $^{40}Ar/^{39}Ar$ date of 75 Ma. [Note: $^{40}Ar/^{39}Ar$ (argon-40/argon-39) is a method for determining the age of igneous rocks based on the slow radioactive decay of the naturally occurring isotope potassium-40 into argon-40.].

Geohydrology of the Hookers Hot Springs area

As a consequence of its poor cementation and coarse grain size, the conglomerate unit in the Hookers Hot Springs area is porous and permeable. The unit hosts approximately 20 springs in the study area (Figure 1). The simplest explanation for the abundance of springs in basin-filling sediments near and north of Hookers Hot Springs is that the conglomerate unit contains much groundwater, and this groundwater is driven to the surface by pressure (hydrostatic head) resulting from recharge in the eastern, elevated side of the basin on the flank of the Winchester Mountains. Basically, the basin is like a tilted bowl of sand, with water flowing to the surface at the lowest part of the bowl (and spilling out to the west across bedrock in Hot Springs Canyon).

Most of the springs, and the highest density of springs, are near lower Bass Canyon, in the area where bed dips change along strike. We suggest that enhanced permeability and high spring density in this area is due to structural disruption associated with the along-strike twisting deformation of beds. Small faults and crushed rocks in this zone, expected as a consequence of deformation where bedding dips reverse direction along strike, is not apparent but may be concealed by abundant disaggregated conglomerate and derivative soil.

Hookers Hot Springs consists of one hot and one cold spring, with the two only ~10 m apart. The only other thermal spring is ~1 km due north of Hookers Hot Springs, and

it is only a very slightly warm seep. Thus, of ~20 springs in the area, only one is a significant hot spring. The most obvious potential source of thermal water in the area is the fault along the west side of the basin, which should provide a conduit for water flow to great depths (~1-3 km) where temperatures are naturally elevated. However, the four springs that are on or near the fault are not thermal springs. Heating due to magma intrusion in the past 1-2 million years is another potential source of heat, but young igneous rocks have not been identified in the area. In conclusion, we were not able to determine, on the basis of the geology of the area, why Hookers Hot Springs is a thermal spring whereas almost all of the others are not.

References Cited

Burchell, A., 1992, Mid-Tertiary volcanic stratigraphy and petrogenesis; Galiuro Mountains, southeastern Arizona – A field based geochemical reconnaissance: Tucson, University of Arizona, M.S. thesis, 156 p.

Burtell, R.T., 1989, Geochemistry and occurrence of ground water in the Allen Flat basin, Arizona: Tucson, University of Arizona M.S. thesis, 163 p.

Creasey, S.C., Jinks, J.E., Williams, F.E. and Meeves, H.C., 1981, Mineral resources of the Galiuro Wilderness and contiguous Further Planning Areas, Arizona: U.S. Geological Survey Bulletin 1490, 94 p., 2 sheets, scale 1:62,500.

Cunningham, E.E.B., Long, A., Eastoe, C. and Bassett, R.L., 1998, Migration of recharge waters downgradient from the Santa Catalina Mountains into the Tucson basin aquifer, Arizona, USA: Hydrogeology Journal, v. 6, p. 94-103.

Davis, G.H. and Hardy, J.J., Jr., 1981, The Eagle Pass detachment, southeastern Arizona; product of mid-Miocene listric(?) normal faulting in the southern Basin and Range: Geological Society of America Bulletin, v. 92, p. 749-762.

Dickinson, W.R., 1991, Tectonic setting of faulted Tertiary strata associated with the Catalina core complex in southern Arizona: Geological Society of America, Special Paper 264, 106 p., with map, scale 1:125,000.

Dickinson, W.R. and Shafiqullah, M., 1989, K-Ar and F-T ages for syntectonic mid-Tertiary volcanosedimentary sequences associated with the Catalina core complex and San Pedro trough in southern Arizona: Isochron/West, n. 52, p. 15-27.

Dickinson, W.R., Goodlin, T. C., Grover, J. A., Mark, R. A. and Shafiqullah, M., 1987, Low-angle normal-fault system along the range front of the southwestern Galiuro Mountains in southeastern Arizona: Geology, v. 15, p. 727-730.

Eastoe, C.J., Gu, A. and Long, A., 2004, The origins, ages, and flow paths of groundwater in Tucson basin: Results of a study of multiple isotope systems, in Hogan, J.F., Phillips, F.M., and Scanlon, B.R., eds., Groundwater recharge in a desert environment: The southwestern United States: American Geophysical Union, Water Science and Application, v. 9, p. 217-234; DOI: 10.1029/WS009

Goodlin, T.C. and Mark, R.A., 1987, Tectonic implications of stratigraphy and structure of Cretaceous rocks and overlying mid-Tertiary cover in Hot Springs Canyon, Galiuro Mountains, southeastern Arizona, in Dickinson, W.R. and Klute, M.A., eds., Mesozoic rocks of southern Arizona and adjacent areas, p.177-188.

Love, D.S., Gootee, B.F., Cook, J.P., Mahan, M.K. and Spencer, J.E., 2014, An investigation of thermal springs throughout Arizona: Geochemical, isotopic, and geological characterization, Arizona Basin and Range Province: Arizona Geological Survey Open-File Report 14-06, 131 p., with appendices.

Richard, S.M., Reynolds, S.J., Spencer, J.E. and Pearthree, P.A., 2000, Geologic map of Arizona: Arizona Geological Survey Map 35, scale 1:1,000,000.

Spencer, J.E. and Reynolds, S.J., 1989, Middle Tertiary tectonics of Arizona and the Southwest, in Jenney, J.P., and Reynolds, S.J., eds., Geologic evolution of Arizona: Arizona Geological Society Digest, v. 17, p. 539-574.

Appendix 1. Hookers Hot Springs map unit descriptions

Qs – Surficial deposits, undivided (Quaternary) – Unlithified streambed sediments and incised soil and alluvial deposits on the flanks of streambeds.

Qtc – Hillslope talus and colluvium – Talus on steep slopes, and unsorted hillside deposits that have not been sorted by alluvial processes and have not been displaced significantly from bedrock sources.

Tcg – Conglomerate and conglomeratic sandstone (Oligocene to lower Miocene) - Conglomerate and pebbly lithic sandstone containing pebbles, cobbles, and locally boulders of mafic, intermediate, and felsic volcanic rocks in poorly sorted, medium- to coarse-grained, lithic sandstone matrix. The unit is thick-bedded, weathers light tan, and forms resistant ledges although some conglomerate intervals high in the section are poorly indurated and form recessive slopes. Conglomerate near the base of the section contains clasts apparently derived from underlying volcanic units, including cobbles and sparse boulders of altered-pyroxene basalt and cobbles of phenocryst-rich and flow-laminated rhyolites. Within the lower 70 to 150 m, basal conglomerate grades upward to an interval of medium- to fine-grained sandstone and pebbly sandstone that is medium-bedded with local cross bedding. This grades upward into conglomerate and pebbly sandstone in which most of the pebbles and cobbles are of mafic to intermediate volcanic rocks. Felsic volcanic cobbles reappear higher in the section. Generally, pebbles and cobbles in the lower part of the section range from well-rounded to subangular, with subrounded being the mode. Cobbles in the upper part of the exposed section in the northern part of the map area are well-rounded.

Tx – Sedimentary breccia (Oligocene to lower Miocene) – Breccia composed of subangular to subrounded (some rounded) cobbles, pebbles, and boulders of altered-pyroxene basalt, evidently derived from the underlying volcanic unit Tm. The breccia is a local unit, up to 30 m thick. It is massive, showing no internal stratification. It overlies basalt of unit Tm in depositional contact and is overlain depositionally by thick-bedded conglomerate of unit Tcg, which contains mainly basalt cobbles and pebbles but other clast types as well. The breccia and conglomerate both have medium-grained sandy matrix, light tan in color.

Tm – Mafic volcanic rocks (Oligocene to lower Miocene) –Undivided mafic lavas including aphyric basalt or andesite, pyroxene basalt, and olivine basalt. Most of the unit in this map area consists of pyroxene basalt, containing 2-4% light-green-altered phenocrysts, 2-4 mm across, that apparently are pseudomorphs of pyroxene replaced by epidote or uralite. Aphyric, vesicular, mafic lava apparently underlies the pyroxene basalt in the southwesternmost part of the unit and is in fault contact with ash-flow tuff of unit Tt. Olivine basalt, containing iddingsite pseudomorphs after olivine phenocrysts, is present in the extreme north.

Tt – Rhyolite ash-flow tuff (Oligocene) – Phenocryst-rich rhyolite ash-flow tuff, containing 20-30% sanidine phenocrysts (1-4 mm), 1-2% biotite phenocrysts (<1 to 2 mm, rarely 3-4 mm), and 5-10% flattened pumice and volcanic-lithic fragments, in a light-orange-brown groundmass. Sample BJJ-4282 of this unit yielded a $^{40}Ar/^{39}Ar$ radiometric date of 27.28 ± 0.06 Ma (million years old). This date is only 0.6 million years younger than that for the bedded pyroclastic rocks of map unit Tbp, which indicates that the two units and intervening rhyolite are part of the same brief period of igneous activity in this area.

Tr - Flow-banded rhyolite and rhyolite autobreccia (Oligocene) - Flow-banded rhyolite and rhyolite autobreccia with 2-3%, <1mm quartz, <1%, <1mm bioitite, and 1-2%, <1mm sanidine. Locally includes vitrophyre. In some areas autobreccia contains flow-banded and flattened rhyolite clasts. Subvertical flow banding and irregular outcrop areas in southern exposures suggest that this unit is partly intrusive.

Tbp - Bedded pyroclastic rocks (Oligocene) – This unit consists primarily of pale gray, bedded tuff containing 6-10%, <1mm, generally fresh biotite, ~15%, <1mm quartz, and 2-5%, <1mm hornblende. Layering in this unit is defined by minor variations in resistance to weathering and by aligned pits that are not flattened and so can't be interpreted as flattened pumice fragments (hence, no eutaxitic foliation, but rather bedding). Locally the unit is interlayered with volcanic-lithic conglomerate in which clasts contain much less biotite and hornblende. Sample 3-19-14-2 (plotted on figure 1 as JES-14-591) of this unit yielded a $^{40}Ar/^{39}Ar$ radiometric date of 27.88 ± 0.02 Ma (million years old).

Tap - Porphyritic andesite (Turkey-Track porphyry) (Oligocene) – Rocks of this unit commonly contain 40-60%, <25 mm plagioclase in dark gray matrix. Some rocks of this unit lack magacrysts but are otherwise similar.

Kc - Sandstone and conglomerate of the Cascabel Formation (upper Cretaceous) - Dark reddish brown, interbedded sandstone and siltstone, and dark reddish brown, matrix supported conglomerate with high silt content. Subrounded to subangular cobbles in conglomerate consist

at least locally of primarily volcanic rocks. Some sandstone is quartz rich.

Km - Muleshoe volcanics (upper Cretaceous) – Gray to tan to brown volcanic rocks with up to 4%, <1mm biotite, up to 8%, <2mm sanidine, and up to 15%, <2mm plagioclase (mostly acicular and generally altered). Sample 3-19-14-2 (plotted on figure 1 as JES-14-583) of this unit yielded a $^{40}Ar/^{39}Ar$ radiometric date of 74.79 ± 0.39 Ma (million years old).

TKsv - Volcanic and sedimentary rocks, undivided (upper Cretaceous to lower Miocene) – Rocks of the Muleshoe volcanics, Cascabel Formation, and porphyritic andesite, undivided.

$^{40}Ar/^{39}Ar$ Geochronology Results from the Galiuro and Muleshoe Volcanics

By

Lisa Peters

SEPTEMBER 8, 2015

Prepared for
Jon Spencer
Arizona Geological Survey
416 W. Congress
Tucson, Arizona 85701

NEW MEXICO
GEOCHRONOLOGY RESEARCH LABORATORY
(NMGRL)

CO-DIRECTORS

DR. MATTHEW T. HEIZLER

DR. WILLIAM C. MCINTOSH

LABORATORY TECHNICIAN

LISA PETERS

Introduction

This report contains data from three samples that were submitted by Jon Spencer from the Galiuro Mountains in Arizona (3-19-14-2, 3-18-14-4 and BJJ-4282). Sample BJJ-4282 was analyzed using sanidine while the other two were analyzed with biotite.

$^{40}Ar/^{39}Ar$ Analytical Methods and Results

Mineral separates were prepared by crushing, treating with dilute HF or dilute HCL, density separation in lithium metatungstate heavy liquid, and hand-picking. The mineral separates and monitors (Fish Canyon tuff sanidine, 28.201 Ma, Kuiper et al., 2008) were loaded into aluminum discs and irradiated for 8 (275) or 16 (276) hours at the USGS TRIGA reactor in Denver Colorado.

The samples were step-heated or fused with a Photon Machines CO_2 laser or diode laser and analyzed with a Thermo Argus VI mass spectrometer. Abbreviated analytical methods for the dated samples are given in Table 1, and details of the overall operation of the New Mexico Geochronology Research Laboratory is provided in the Appendix. The age results are summarized in Table 1 and the argon isotopic data are given in Tables 2 and 3.

Thirteen single crystals of sanidine were analyzed from BJJ-4282. All thirteen were used to calculate a weighted mean age of 27.28±0.06 Ma. Radiogenic yields ranged from 78.5% to 94.8% and K/Ca values ranged between 6.2-19.3.

Sample 3-19-14-2 was analyzed using a bulk biotite separate. The first heating step was anomalously young. The following ~21% of the heating schedule reveals decreasing apparent ages (29.35 Ma to 28.06 Ma) and increasing radiogenic yields (69.4% to 95.1%). The following 77.3% of the age spectrum is used to calculate a weighted mean age of 27.88±0.02 Ma. Inverse isochron analysis of steps C-M reveal an isochron age of 27.55±0.11 Ma with an $^{40}Ar/^{36}Ar$ intercept of 417±30. Well above the atmospheric intercept of 295.5. We note that points C-M are clustered near the x axis.

Sample 3-18-14-4 biotite was analyzed first with a bulk aliquot made of many crystals. This aliquot revealed a somewhat disturbed age spectrum with increasing apparent ages (48.15 Ma to 75.47 Ma) and radiogenic yields (70.8% to 97.9%) over the initial ~30% of the age spectra. A weighted mean age of 75.35±0.23 Ma (MSWD=187) is calculated from the following 70.8% of the ^{39}Ar released. Five more single crystals of biotite were analyzed. Three aliquots revealed age spectra similar to the bulk analysis, with increasing radiogenic yields and apparent ages over the early portions of the age spectra followed by a relatively concordant portion. Weighted mean ages are calculated for these concordant portions of the age spectra. Two aliquots revealed disturbed age spectra; one hump-shaped and the other stair-step up throughout the entire age spectrum. An apparent age of 74.79±0.39 Ma is calculated from the weighted mean ages assigned to the four best behaved age spectra.

Discussion

The weighted mean age assigned to the rhyolite lava BJJ-4282 (27.28±0.06 Ma) is interpreted to be both precise and reliable. We have assigned the weighted mean calculated from 3-19-14-2 biotite (27.88±0.02 Ma) as the preferred eruption age for this pryroclastic rock. The isochron age is well above the atmospheric intercept but, due to uniformly high (>95%) radiogenic yields and therefore clustering of the points near the x axis, we have not chosen to use this age. We also note that the integrated age (27.97±0.02 Ma) and the weighted mean age (27.88±0.02 Ma) nearly agree within the quoted error. The age assigned to 3-18-14-4 (74.79±0.39 Ma) is somewhat less precise than the others in this report and we do note that the increasing apparent ages and radiogenic yields revealed by the early heating steps are strongly suggestive of alteration and Ar loss. We do feel that the assigned weighted mean age (74.79±0.39 Ma) provides an accurate eruption age within the quoted error.

References Cited

Kuiper, K. F., Deino, A., Hilgen, F. J., Krijgsman, W., Renne, P. R., and Wijbrans, J. R., 2008, Synchronizing rock clocks of earth history: Science, v. 320, p. 500-504.

Min, K., Mundil, R., Renne, P. L., and Ludwig, K.R., 2000, A test for systematic errors in $^{40}Ar/^{39}Ar$ geochronology through comparison with U/Pb analysis of a 1.1-Ga rhyolite: Geochimica et Cosmochimica Acta, v. 64, p. 73-98.

Taylor, J.R., 1982. An Introduction to Error Analysis: The Study of Uncertainties in Physical Measurements,. Univ. Sci. Books, Mill Valley, Calif., 270 p.

Table 1. Summary of $^{40}Ar/^{39}Ar$ results and analytical methods

Sample	Lab #	Irradiation	mineral	age analysis	steps/analyses	Age	±2σ	MSWD	comments
BJJ-4282	63724	276	sanidine	laser fusion	15	27.28	0.06	8.59	weighted mean
3-19-14-2	63326	275	biotite	step-heat	6	27.88	0.02	5.35	weighted mean
3-18-14-4	63690	276	biotite	step-heat	4	74.79	0.39	15.4	weighted mean

Sample preparation and irradiation:
Minerals separated with standard heavy liquid, Franz Magnetic and hand-picking techniques.
Samples in NM-275 were irradiated for 8 hours while those in 276 were irradiated in a machined Aluminum tray for 16 hours.
All were irradiated in C.T. position, USGS TRIGA, Denver, Colorado.
Neutron flux monitor Fish Canyon Tuff sanidine (FC-2). Assigned age = 28.201 Ma (Kuiper et al., 2008).

Instrumentation:
Total fusion monitor analyses performed on a Argus VI mass spectrometer on line with automated all-metal extraction system. System = Jan
Step-heat analyses performed on a Argus VI mass spectrometer on line with automated all-metal extraction system. System = Obama
Multi-collector configuration: 40Ar-H1, 39Ar-Ax, 38Ar-L1, 37Ar-L2, 36Ar-CDD
Flux monitors fused with a Photon Machines Inc. CO_2 laser. Groundmass concentrate and biotite step-heated with a Photon Machine Inc. Diode laser.

Analytical parameters:
Sensitivity for the Argus VI with the Diode laser (step-heated samples) is 9.84e-17 moles/fA.
Sensitivty for the Argus VI with the CO2 laser (fused monitors)is 4.62 e-17 moles/fA.
Typical system blank and background was 194, 1.76, 0.197, 4.92, 0.59 x 10^{-18} moles at masses 40, 39, 38, 37 and 36, respectively for the laser analyses.
J-factors determined by CO_2 laser-fusion of 6 single crystals from each of 8 radial positions around the irradiation tray.
Decay constants and isotopic abundances after Minn et al., (2000).

Table 2. $^{40}Ar/^{39}Ar$ analytical data.

ID	$^{40}Ar/^{39}Ar$	$^{37}Ar/^{39}Ar$	$^{36}Ar/^{39}Ar$ (x 10^{-3})	$^{39}Ar_K$ (x 10^{-15} mol)	K/Ca	$^{40}Ar^*$ (%)	Age (Ma)	±1σ (Ma)
BJJ-4282, san, J=0.0038317±0.03%, D=1±0, NM-276J, Lab#=63724								
08	4.310	0.0308	1.434	1.205	16.6	90.0	27.02	0.04
14	4.539	0.0264	2.128	0.712	19.3	86.0	27.18	0.06
05	4.731	0.0430	2.769	0.934	11.9	82.6	27.21	0.06
03	4.237	0.0701	1.096	0.986	7.3	92.3	27.23	0.04
09	4.436	0.0446	1.745	2.159	11.4	88.3	27.26	0.03
11	4.130	0.0343	0.7058	1.472	14.9	94.8	27.26	0.03
02	4.191	0.0260	0.9122	3.539	19.7	93.4	27.26	0.02
12	4.229	0.0820	1.030	1.236	6.2	92.8	27.31	0.03
10	5.001	0.0392	3.623	1.207	13.0	78.5	27.33	0.06
04	4.351	0.0340	1.386	0.714	15.0	90.5	27.40	0.05
06	4.282	0.0592	1.142	0.727	8.6	92.0	27.44	0.05
07	4.282	0.0515	1.121	0.886	9.9	92.2	27.47	0.04
15	4.216	0.0717	0.8851	0.626	7.1	93.7	27.51	0.05
Mean age ± 2σ		**n=13**	**MSWD=9.98**		**12.4 ±9.0**		**27.28**	**0.06**

Notes:
Isotopic ratios corrected for blank, radioactive decay, and mass discrimination, not corrected for interfering reactions.
Errors quoted for individual analyses include analytical error only, without interfering reaction or J uncertainties.
Mean age is weighted mean age of Taylor (1982). Mean age error is weighted error of the mean (Taylor, 1982), multiplied by the root of the MSWD where MSWD>1, and also incorporates uncertainty in J factors and irradiation correction uncertainties.
Decay constants and isotopic abundances after Minn et al., (2000).
symbol preceding sample ID denotes analyses excluded from mean age calculations.
Ages calculated relative to FC-2 Fish Canyon Tuff sanidine interlaboratory standard at 28.201Ma
Decay Constant (LambdaK (total)) = 5.543e-10/a
Correction factors:
$(^{39}Ar/^{37}Ar)_{Ca}$ = 0.0007064 ± 4e-06
$(^{36}Ar/^{37}Ar)_{Ca}$ = 0.0002731 ± 0
$(^{38}Ar/^{39}Ar)_K$ = 0.01261
$(^{40}Ar/^{39}Ar)_K$ = 0.00808 ± 0.00041

Table 3. $^{40}Ar/^{39}Ar$ analytical data.

	ID	Power (Watts)	$^{40}Ar/^{39}Ar$	$^{37}Ar/^{39}Ar$	$^{36}Ar/^{39}Ar$ (x 10^{-3})	$^{39}Ar_K$ (x 10^{-15} mol)	K/Ca	$^{40}Ar^*$ (%)	^{39}Ar (%)	Age (Ma)	±1σ (Ma)
	3-19-14-2, bi, 2.11 mg, J=0.0019207±0.02%, D=1±0, NM-275D, Lab#=63549-01										
Xi	A	1	68.75	0.2333	208.0	0.934	2.2	10.6	1.3	25.44	0.39
Xi	B	2	12.13	0.0151	12.55	0.800	33.9	69.4	2.4	29.35	0.09
X	C	3	9.213	0.0589	3.112	4.26	8.7	90.0	8.4	28.92	0.02
X	D	3	8.589	0.1300	1.602	4.09	3.9	94.5	14.1	28.33	0.02
X	E	4	8.455	0.0591	1.391	4.77	8.6	95.1	20.8	28.06	0.01
	F	4	8.347	0.0994	1.198	7.19	5.1	95.8	30.9	27.89	0.01
	G	5	8.238	0.0181	0.8495	11.45	28.1	96.9	46.9	27.85	0.01
	H	5	8.222	0.0115	0.7490	7.86	44.4	97.2	57.9	27.90	0.01
	I	5	8.218	0.0260	0.7405	7.80	19.6	97.3	68.9	27.89	0.01
	J	6	8.199	0.0120	0.6834	14.77	42.3	97.5	89.6	27.88	0.01
	K	8	8.275	0.0122	0.9183	6.11	41.9	96.6	98.1	27.91	0.01
X	L	15	8.478	0.0228	1.437	1.300	22.4	94.9	100.0	28.08	0.04
X	M	10	8.526	3.457	3.907	0.021	0.15	89.7	100.0	26.75	2.12
	Integrated age ± 2σ			n=13		71.3	12.7	K2O=6.76%		27.97	0.01
	Plateau ± 2σ steps F-K			**n=6**	**MSWD=5.34**	**55.2**	**31.6 ±31.4**		**77.3**	**27.88**	**0.02**
	Isochron±2σ steps C-M			n=11	MSWD=28.80		$^{40}Ar/^{36}Ar$= 417±30			27.55	0.11
	3-18-14-4, Biotite, 2.35 mg, J=0.0039066±0.02%, D=1±0, NM-276G, Lab#=63690-01										
X	A	1	9.633	0.2134	9.547	4.84	2.4	70.8	3.3	48.15	0.10
X	B	1	10.19	0.6453	3.867	3.84	0.79	89.2	5.9	63.91	0.08
X	C	1	10.51	0.4710	2.065	5.54	1.1	94.5	9.6	69.70	0.05
X	D	1	10.96	0.2968	1.405	8.58	1.7	96.4	15.4	74.05	0.04
X	E	2	11.03	0.1379	0.8809	20.0	3.7	97.7	28.9	75.47	0.02
	F	2	10.97	0.0225	0.4365	18.94	22.7	98.8	41.7	75.91	0.02
	G	2	10.89	0.0272	0.3227	14.31	18.8	99.1	51.4	75.59	0.02
	H	2	10.83	0.0440	0.2864	12.60	11.6	99.2	59.9	75.28	0.03
	I	2	10.80	0.0371	0.2691	13.48	13.8	99.2	69.0	75.06	0.02
	J	3	10.79	0.0284	0.2283	16.53	17.9	99.3	80.2	75.09	0.02
	K	4	10.80	0.0471	0.2186	25.8	10.8	99.4	97.7	75.20	0.02
	L	4	10.87	0.1015	0.2415	1.796	5.0	99.4	98.9	75.63	0.11
	M	5	10.77	0.0538	0.3429	1.288	9.5	99.0	99.7	74.75	0.12
X	N	7	11.51	0.2496	0.9106	0.353	2.0	97.8	100.0	78.79	0.49
X	O	21	20.84	-2.0677	11.54	0.027	-	82.8	100.0	119.17	7.76
X	P	23	15.61	-1.6456	15.69	0.009	-	69.2	100.0	75.61	16.78
	Integrated age ± 2σ			n=16		147.9	4.9	K2O=6.19		73.92	0.04
	Plateau ± 2σ steps F-M			**n=8**	**MSWD=187.07**	**104.739**	**5.530±5.726**		**70.8**	**75.35**	**0.23**
	Isochron±2σ steps D-P			n=13	MSWD=243.37		$^{40}Ar/^{36}Ar$= 306±59			75.29	0.32

	ID	Power (Watts)	$^{40}Ar/^{39}Ar$	$^{37}Ar/^{39}Ar$	$^{36}Ar/^{39}Ar$ (x 10^{-3})	$^{39}Ar_K$ (x 10^{-15} mol)	K/Ca	$^{40}Ar^*$ (%)	^{39}Ar (%)	Age (Ma)	±1σ (Ma)
	3-18-14-4, Biotite, .36 mg, J=0.0039066±0.02%, D=1±0, NM-276G, Lab#=63690-02										
X	A	1	13.26	0.1416	23.10	1.01	3.6	48.6	8.8	45.49	0.14
X	B	1	11.08	-0.0884	2.322	0.796	-	93.7	15.7	72.76	0.08
X	C	1	11.71	-0.0145	1.197	1.11	-	96.9	25.3	79.41	0.06
X	D	1	11.99	0.0563	0.7645	1.30	9.1	98.1	36.6	82.24	0.05
X	E	2	12.14	-0.0279	0.7701	2.32	-	98.1	56.8	83.20	0.03
X	F	2	12.44	0.0728	0.9599	1.05	7.0	97.7	66.0	84.90	0.06
X	G	2	12.78	-0.1567	1.029	0.648	-	97.5	71.6	86.93	0.10
X	H	2	12.82	0.3343	1.099	0.463	1.5	97.6	75.6	87.42	0.14
X	I	2	12.69	0.1726	1.357	0.347	3.0	96.9	78.6	85.88	0.17
X	J	3	12.53	-0.4259	1.199	0.329	-	96.8	81.5	84.77	0.18
X	K	4	11.52	0.0410	0.4695	1.44	12.4	98.8	94.0	79.58	0.04
X	L	4	11.57	0.4209	0.3716	0.507	1.2	99.3	98.4	80.36	0.11
X	M	5	11.81	-0.2544	0.5127	0.149	-	98.5	99.7	81.31	0.37
X	N	7	10.43	-0.7562	1.816	0.032	-	94.2	100.0	68.92	1.45
X	O	21	43.38	-11.8885	86.23	0.006	-	38.9	100.1	116.06	12.70
X	P	23	-11.0703	9.009	-29.7974	-0.006	0.057	14.7	100.0	-11.74	4.54
	Integrated age ± 2σ			n=16		11.5	28.9		K2O=3.14	78.80	0.06
	3-18-14-4, Biotite, .31 mg, J=0.0039066±0.02%, D=1±0, NM-276G, Lab#=63690-03										
Xi	A	1	9.593	2.327	6.273	0.933	0.22	82.6	12.4	55.86	0.08
Xi	B	1	10.01	1.220	1.842	0.994	0.42	95.5	25.7	67.14	0.06
X	C	1	10.20	0.0237	0.6148	1.12	21.5	98.2	40.6	70.26	0.05
X	D	1	10.52	-0.0772	0.5112	0.842	-	98.4	51.8	72.58	0.06
X	E	2	10.51	0.0565	0.3342	2.34	9.0	99.0	83.0	72.95	0.03
X	F	2	10.75	0.1591	0.2747	0.892	3.2	99.3	94.9	74.78	0.06
X	G	2	10.84	-0.3300	0.3601	0.192	-	98.7	97.4	74.94	0.27
Xi	H	2	9.935	-0.4427	0.6527	0.027	-	97.7	97.8	68.12	1.68
Xi	I	2	10.93	-0.2566	0.9031	0.019	-	97.4	98.0	74.64	2.58
Xi	J	3	8.568	3.958	0.7428	0.024	0.13	101.1	98.4	61.08	1.74
Xi	K	4	12.22	-0.3609	0.7064	0.069	-	98.0	99.3	83.71	0.77
Xi	L	4	6.509	2.262	0.9900	0.015	0.23	97.8	99.5	45.03	2.20
Xi	M	5	10.54	7.013	1.350	0.018	0.073	101.8	99.7	75.48	2.74
Xi	N	7	11.42	-4.1394	1.841	0.016	-	92.2	99.9	73.59	2.93
Xi	O	21	20.01	9.784	22.52	0.006	0.052	70.8	100.0	99.34	11.53
Xi	P	23	-277.2260	-136.6886	-961.8844	0.000	-	2.0	100.0	-36.95	127.72
	Integrated age ± 2σ			n=16		7.51	1.0		K2O=2.38	69.91	0.07

	ID	Power (Watts)	$^{40}Ar/^{39}Ar$	$^{37}Ar/^{39}Ar$	$^{36}Ar/^{39}Ar$ (x 10^{-3})	$^{39}Ar_K$ (x 10^{-15} mol)	K/Ca	$^{40}Ar^*$ (%)	^{39}Ar (%)	Age (Ma)	±1σ (Ma)
	3-18-14-4, Biotite, .46 mg, J=0.0039066±0.02%, D=1±0, NM-276G, Lab#=63690-04										
Xi	A	1	11.28	1.218	8.661	0.835	0.42	78.1	5.7	62.00	0.10
Xi	B	1	10.39	0.3330	1.434	0.831	1.5	96.1	11.5	70.05	0.07
Xi	C	1	10.67	-0.0601	0.5580	1.07	-	98.3	18.8	73.55	0.06
Xi	D	1	10.71	0.0539	0.3632	1.11	9.5	99.0	26.4	74.27	0.05
X	E	2	10.71	0.0541	0.2960	3.43	9.4	99.2	50.0	74.44	0.02
	F	2	10.76	0.0698	0.1799	2.87	7.3	99.5	69.8	75.02	0.02
	G	2	10.77	0.0211	0.1367	1.65	24.2	99.6	81.2	75.16	0.04
	H	2	10.80	0.0246	0.1139	1.78	20.7	99.6	93.4	75.40	0.04
	I	2	10.81	0.0139	0.1007	0.584	36.6	99.7	97.4	75.49	0.09
Xi	J	3	10.97	0.3692	0.2338	0.079	1.4	99.6	98.0	76.50	0.63
Xi	K	4	10.67	-1.0508	0.1250	0.129	-	98.8	98.9	73.82	0.38
Xi	L	4	12.19	-0.4599	0.5146	0.038	-	98.4	99.1	83.75	1.46
Xi	M	5	10.56	-0.7585	0.2728	0.112	-	98.6	99.9	72.96	0.43
Xi	N	7	12.77	-1.0840	1.444	0.009	-	95.6	100.0	85.23	5.88
Xi	O	21	20.42	20.96	15.01	0.006	0.024	86.7	100.0	124.26	12.32
	Integrated age ± 2σ			n=16		14.5	4.4		K2O=3.11	73.81	0.05
	Plateau ± 2σ	**steps F-I**		**n=4**	**MSWD=32.06**	**6.89**	**17.3 ±12.1**		**47.4**	**75.15**	**0.20**
	Isochron±2σ	steps E-I		n=5	MSWD=2.78		$^{40}Ar/^{36}Ar$=461.4±30.7			75.86	0.09
	3-18-14-4, Biotite, .31 mg, J=0.0039066±0.02%, D=1±0, NM-276G, Lab#=63690-05										
X	A	1	18.40	-17.9158	58.87	0.002	-	-1.9	0.0	-2.42	11.88
X	B	1	116.4	-180.0973	382.4	0.000	-	-9.5	0.0	-71.55	142.92
X	C	1	11.22	0.2777	6.000	0.903	1.8	84.3	9.4	66.49	0.09
X	D	1	10.96	-0.0305	1.189	0.897	-	96.7	18.7	74.24	0.07
X	E	1	10.91	-0.0045	0.6631	0.899	-	98.1	28.0	75.01	0.07
X	F	1	11.00	-0.0407	0.5577	0.892	-	98.4	37.2	75.82	0.07
	G	2	10.87	0.0068	0.4775	2.01	75.1	98.6	58.0	75.13	0.03
	H	2	10.85	0.0531	0.4349	1.17	9.6	98.8	70.2	75.12	0.05
	I	2	10.88	0.0243	0.2489	1.56	21.0	99.3	86.3	75.63	0.04
	J	2	10.89	0.0370	0.2973	1.02	13.8	99.2	96.8	75.64	0.06
X	K	2	11.45	0.0796	0.6060	0.133	6.4	98.4	98.2	78.85	0.39
X	L	3	12.41	0.9659	0.5924	0.042	0.53	99.1	98.6	85.97	1.30
X	M	4	11.47	0.3827	0.5686	0.104	1.3	98.7	99.7	79.24	0.49
X	N	4	8.125	-4.9243	1.141	0.012	-	90.6	99.8	51.72	3.07
X	O	5	13.79	-6.9874	0.3127	0.008	-	95.2	99.9	91.09	6.63
X	P	7	2.886	2.017	3.936	0.005	0.25	66.0	100.0	13.60	4.55
X	Q	21	12.47	23.78	9.517	0.003	0.021	93.7	100.0	83.02	20.89
X	R	23	-17.2449	17.74	-31.1522	-0.002	0.029	38.6	100.0	-48.85	24.98
	Integrated age ± 2σ			n=18		9.66	19.0		K2O=3.06	74.52	0.06
	Plateau ± 2σ	**steps G-J**		**n=4**	**MSWD=47.39**	**5.761**	**6.325±30.504**		**59.6**	**75.34**	**0.29**
	Isochron±2σ	steps A-R		n=18	MSWD=37.86		$^{40}Ar/^{36}Ar$= 62.5±1.4			76.04	0.05

	ID	Power (Watts)	$^{40}Ar/^{39}Ar$	$^{37}Ar/^{39}Ar$	$^{36}Ar/^{39}Ar$ (x 10^{-3})	$^{39}Ar_K$ (x 10^{-15} mol)	K/Ca	$^{40}Ar^*$ (%)	^{39}Ar (%)	Age (Ma)	±1σ (Ma)
	3-18-14-4, Biotite, .67 mg, J=0.0039066±0.02%, D=1±0, NM-276G, Lab#=63690-06										
Xi	A	1	13.29	0.5233	19.50	0.139	0.97	56.9	0.7	53.32	0.42
Xi	B	1	10.50	0.8611	6.429	0.569	0.59	82.5	3.4	60.97	0.12
Xi	C	1	10.27	1.495	4.533	0.501	0.34	88.1	5.8	63.65	0.12
Xi	D	1	10.39	0.7649	2.372	0.751	0.67	93.8	9.3	68.40	0.08
Xi	E	2	10.58	0.2137	1.090	2.26	2.4	97.1	20.1	72.01	0.03
Xi	F	2	10.66	-0.0286	0.6265	1.72	-	98.2	28.3	73.38	0.04
Xi	G	2	10.72	0.0357	0.4842	1.36	14.3	98.6	34.8	74.09	0.04
	H	2	10.81	0.0316	0.4853	1.12	16.1	98.6	40.1	74.67	0.05
	I	2	11.05	0.0936	1.391	10.4	5.5	96.3	89.6	74.56	0.01
X	J	3	10.78	-0.0171	0.1539	1.81	-	99.5	98.2	75.16	0.03
Xi	K	4	10.97	0.2334	0.2037	0.249	2.2	99.6	99.4	76.48	0.22
Xi	L	4	11.68	0.0709	0.6284	0.027	7.2	98.3	99.5	80.33	1.98
Xi	M	5	10.49	6.067	2.867	0.010	0.084	96.5	99.6	71.30	4.84
Xi	N	7	11.86	-2.5032	1.819	0.068	-	93.7	99.9	77.69	0.75
Xi	O	21	27.85	-1.2759	60.90	0.020	-	34.9	100.0	68.25	2.67
Xi	P	23	43.99	17.55	140.2	0.004	0.029	9.2	100.0	28.99	7.68
	Integrated age ± 2σ			n=16		21.0	3.2		K2O=3.08	73.25	0.04
	Plateau ± 2σ	**steps H-I**		**n=2**	**MSWD=3.65**	**11.5**	**6.5 ±7.6**		**54.8**	**74.57**	**0.06**
	Isochron±2σ	steps H-J		n=3	MSWD=34.79		$^{40}Ar/^{36}Ar$=	233.2±3.8		75.14	0.07

Notes:

Isotopic ratios corrected for blank, radioactive decay, and mass discrimination, not corrected for interfering reactions.
Errors quoted for individual analyses include analytical error only, without interfering reaction or J uncertainties.
Integrated age calculated by summing isotopic measurements of all steps.
Integrated age error calculated by quadratically combining errors of isotopic measurements of all steps.
Plateau age is inverse-variance-weighted mean of selected steps.
Plateau age error is inverse-variance-weighted mean error (Taylor, 1982) times root MSWD where MSWD>1.
Plateau error is weighted error of Taylor (1982).
Decay constants and isotopic abundances after Minn et al., (2000).
symbol preceding sample ID denotes analyses excluded from plateau age calculations.
Weight percent K_2O calculated from ^{39}Ar signal, sample weight, and instrument sensitivity.
Ages calculated relative to FC-2 Fish Canyon Tuff sanidine interlaboratory standard at 28.201Ma
Decay Constant (LambdaK (total)) = 5.463e-10/a
Correction factors:

$(^{39}Ar/^{37}Ar)_{Ca}$ = 0.0007064 ± 4e-06
$(^{36}Ar/^{37}Ar)_{Ca}$ = 0.0002731 ± 0
$(^{38}Ar/^{39}Ar)_K$ = 0.01261
$(^{40}Ar/^{39}Ar)_K$ = 0.00808 ± 0.00041

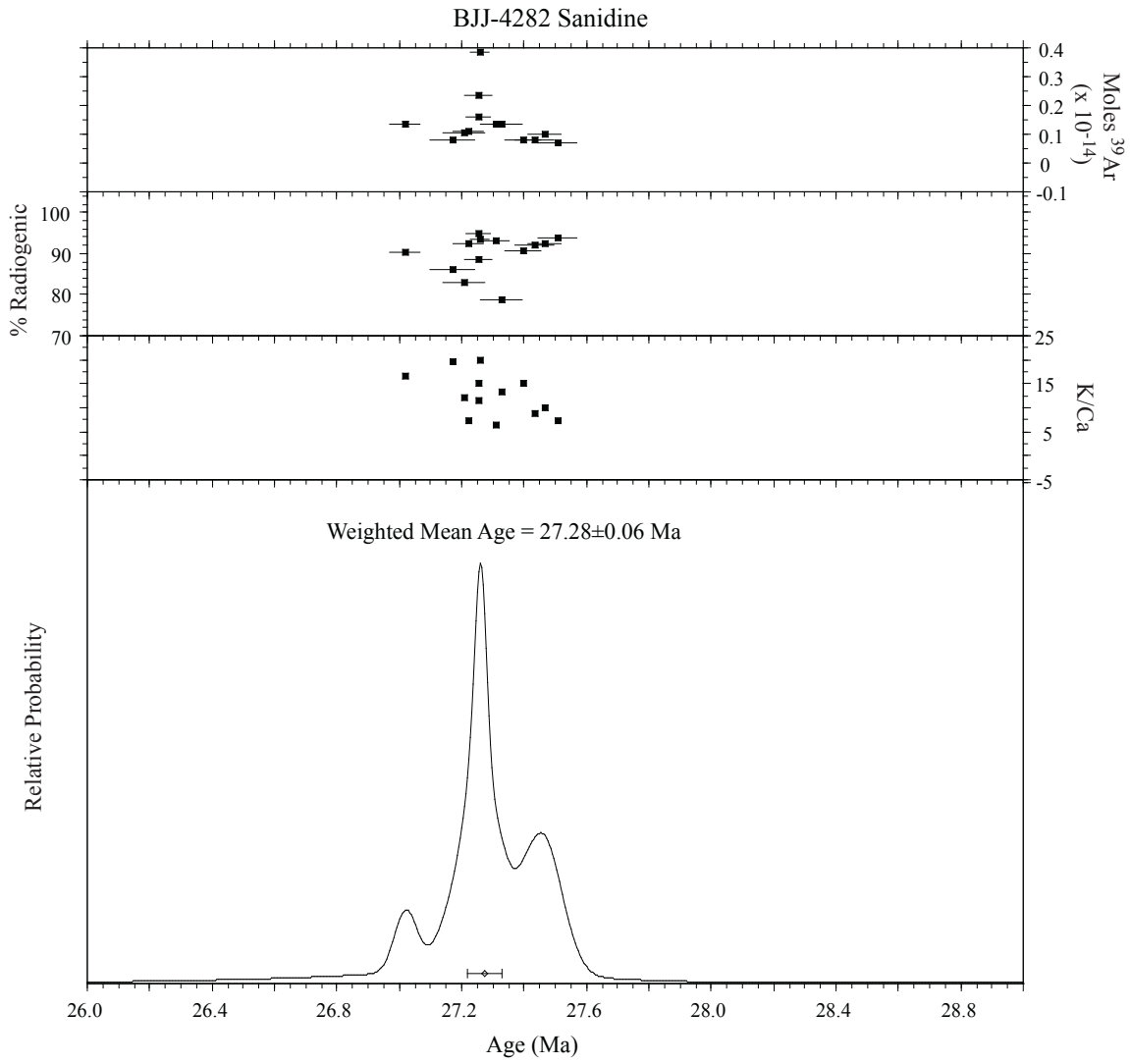
BJJ-4282 Sanidine
Moles ^{39}Ar (x 10^{-14})
0.4
0.3
0.2
0.1
0
-0.1
% Radiogenic
100
90
80
70
K/Ca
25
15
5
-5
Weighted Mean Age = 27.28±0.06 Ma
Relative Probability
26.0
26.4
26.8
27.2
27.6
28.0
28.4
28.8
Age (Ma)

3-19-14-2 Biotite

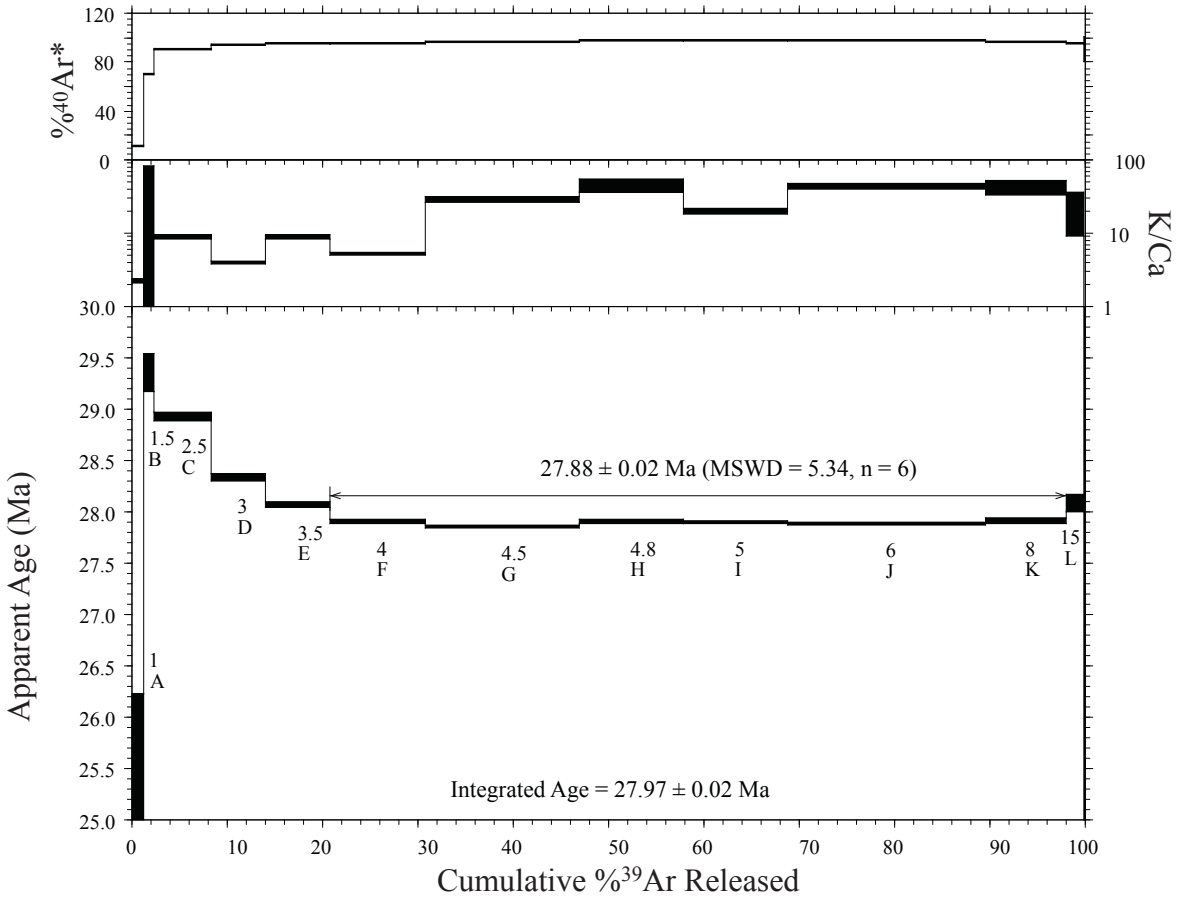

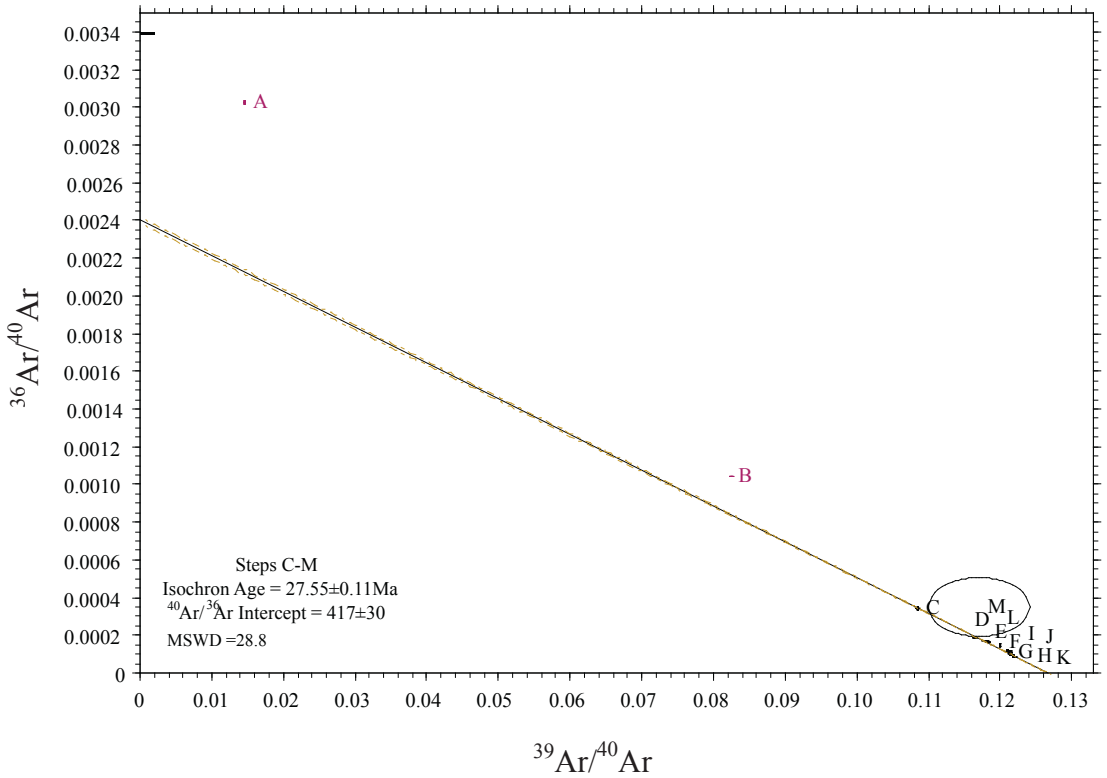

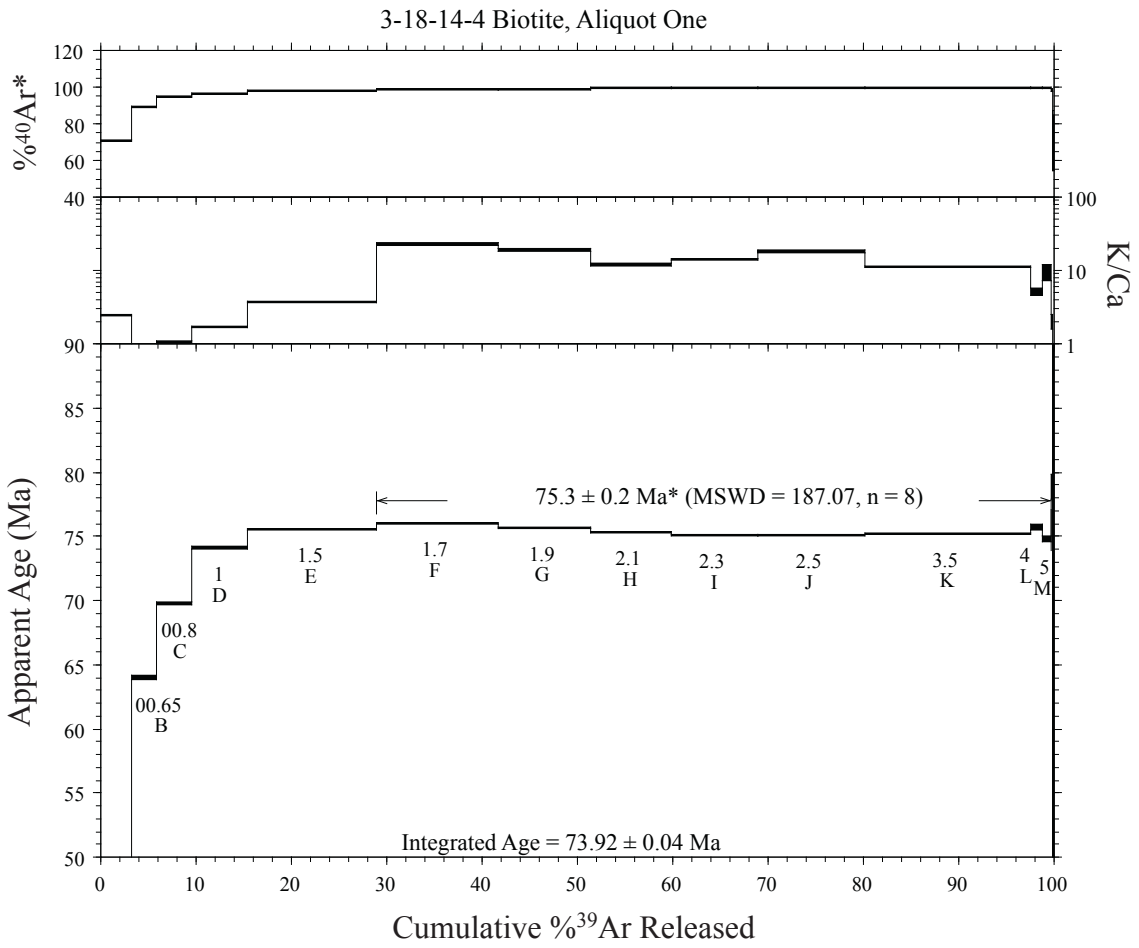
3-18-14-4 Biotite, Aliquot One
%40Ar*
K/Ca
Apparent Age (Ma)
75.3 ± 0.2 Ma* (MSWD = 187.07, n = 8)
00.65 B
00.8 C
1 D
1.5 E
1.7 F
1.9 G
2.1 H
2.3 I
2.5 J
3.5 K
4 L
5 M
Integrated Age = 73.92 ± 0.04 Ma
Cumulative %39Ar Released

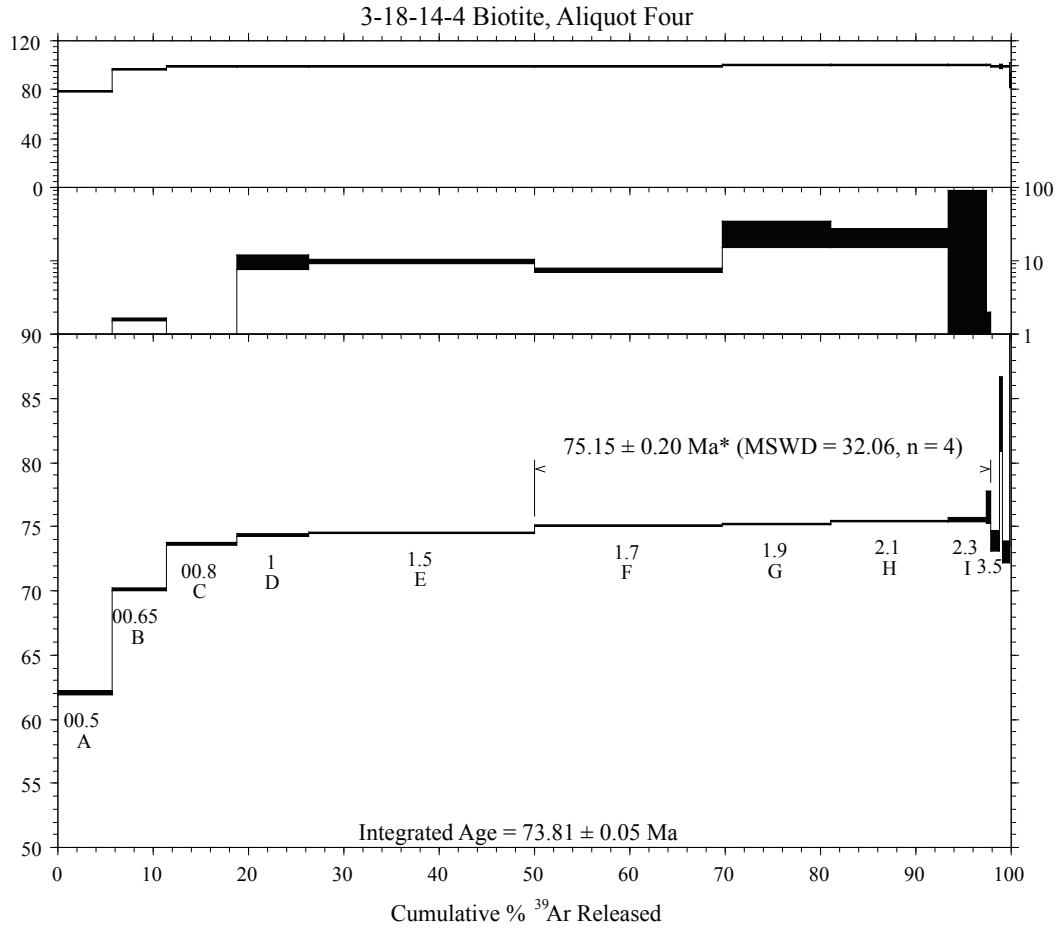
3-18-14-4 Biotite, Aliquot Four
75.15 ± 0.20 Ma* (MSWD = 32.06, n = 4)
00.5 A
00.65 B
00.8 C
1 D
1.5 E
1.7 F
1.9 G
2.1 H
2.3 I
3.5
Integrated Age = 73.81 ± 0.05 Ma
Cumulative % 39Ar Released

3-18-14-4 Biotite, Aliquot Five

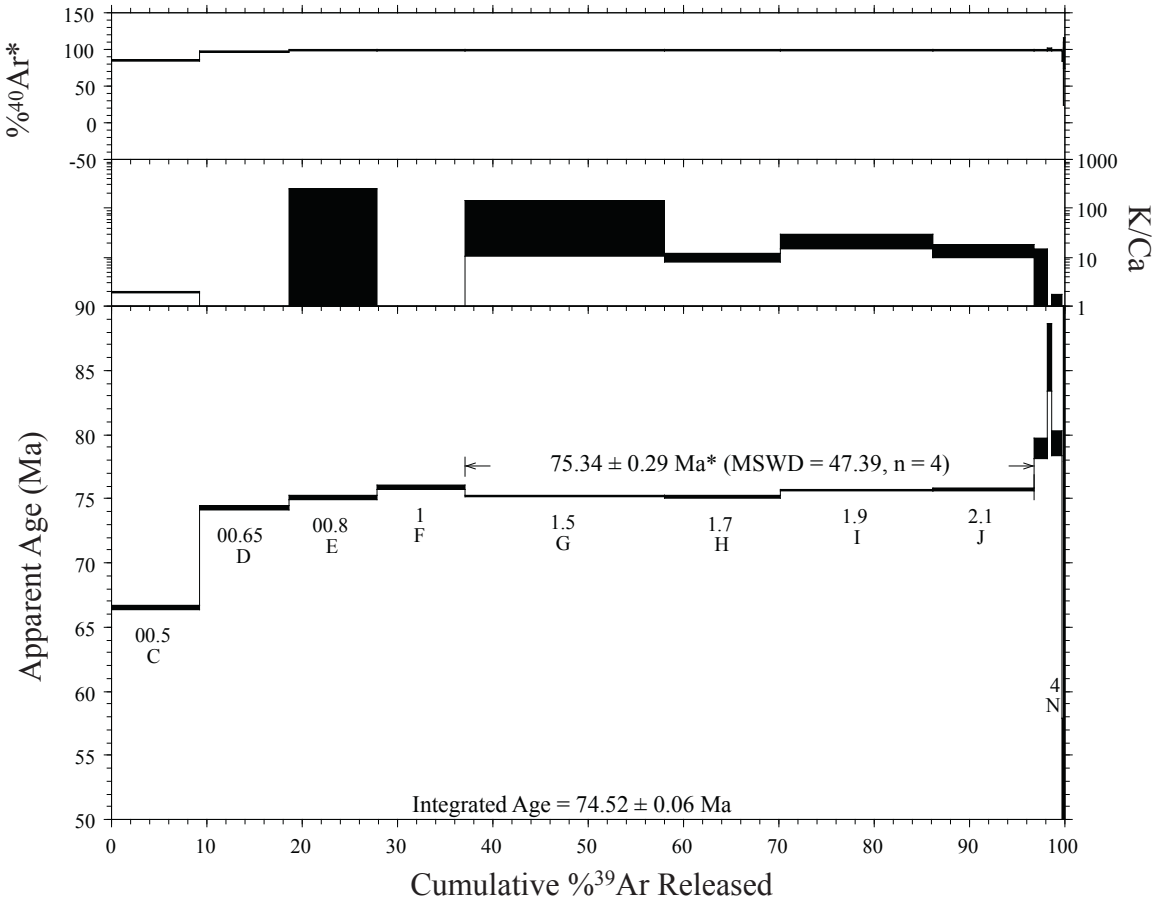

3-18-14-4 Biotite, Aliquot Six

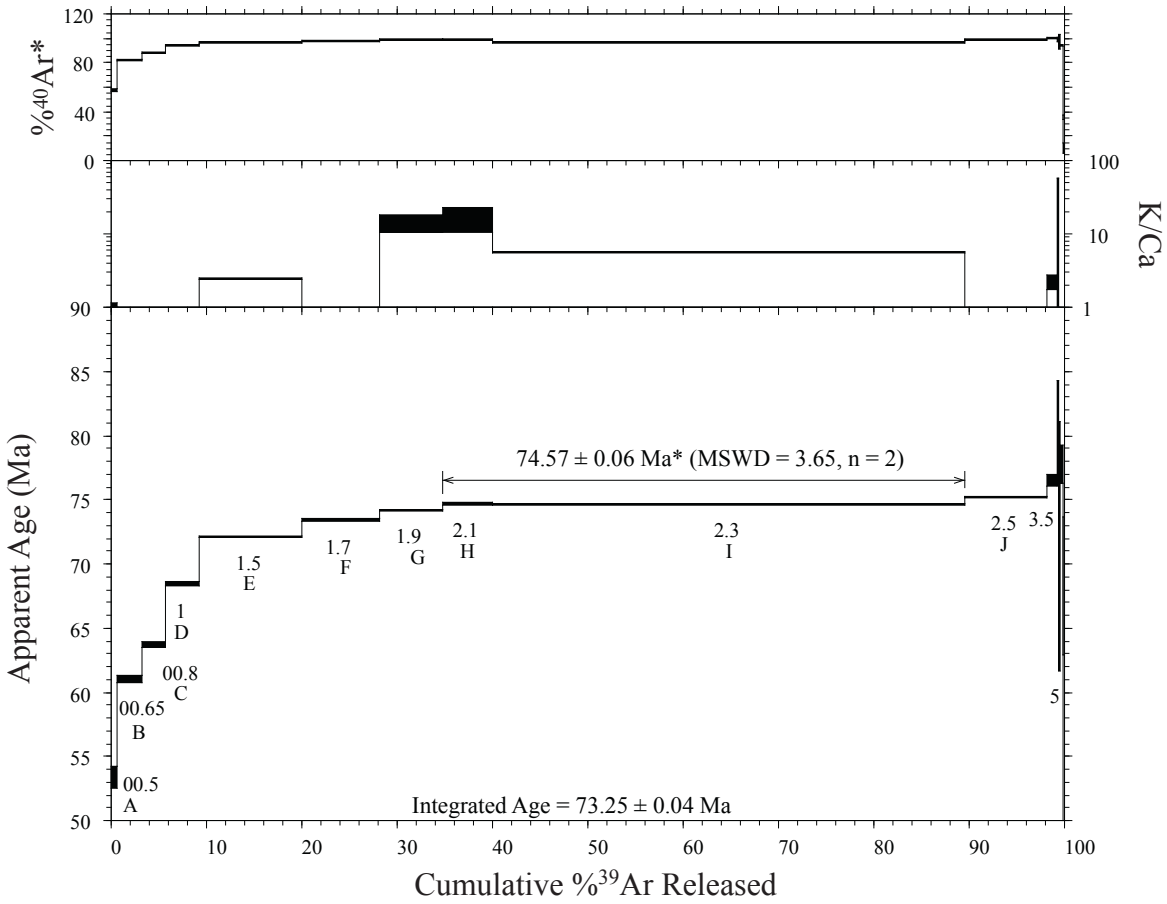

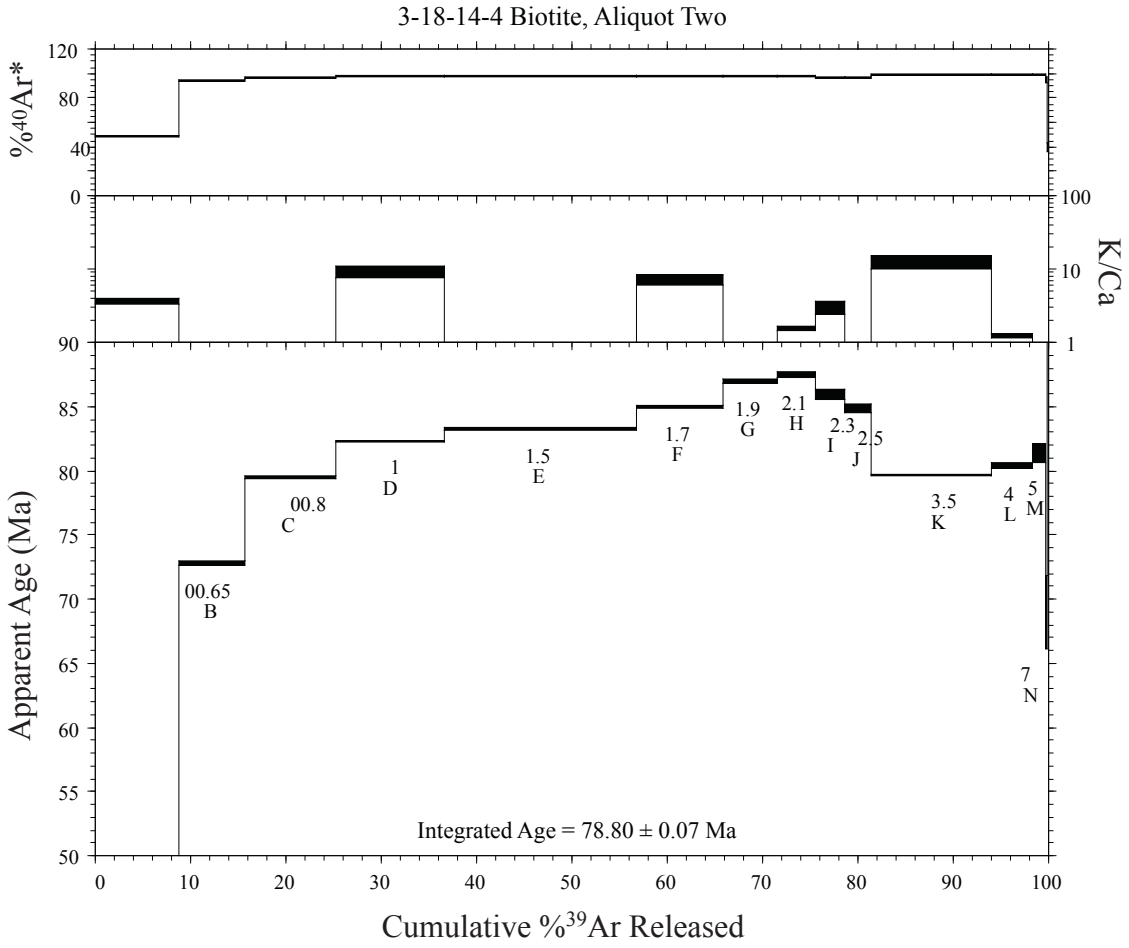
3-18-14-4 Biotite, Aliquot Two
%40Ar*
K/Ca
Apparent Age (Ma)
00.65
B
00.8
C
1
D
1.5
E
1.7
F
1.9
G
2.1
H
2.3
I
2.5
J
3.5
K
4
L
5
M
7
N
Integrated Age = 78.80 ± 0.07 Ma
Cumulative %39Ar Released

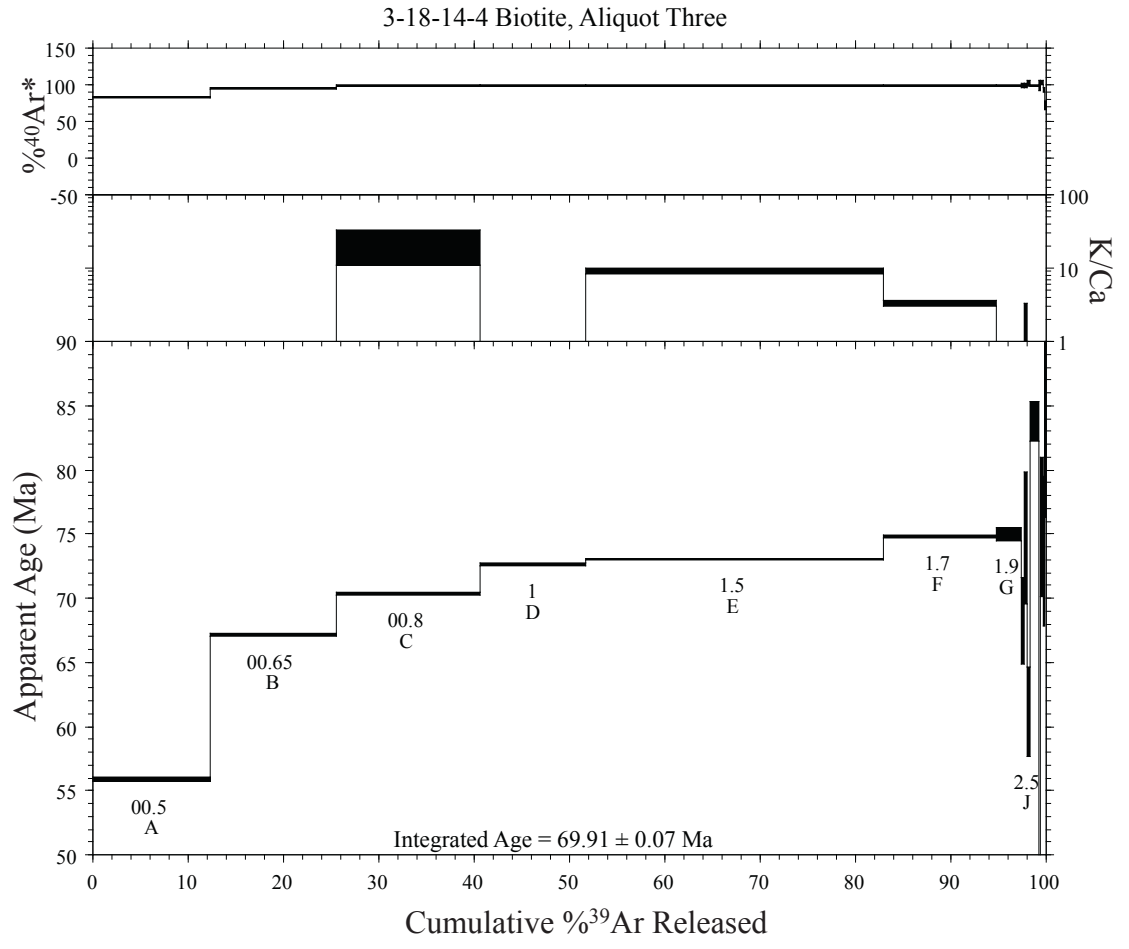
3-18-14-4 Biotite, Aliquot Three
%40Ar*
K/Ca
Apparent Age (Ma)
00.5
A
00.65
B
00.8
C
1
D
1.5
E
1.7
F
1.9
G
2.5
J
Integrated Age = 69.91 ± 0.07 Ma
Cumulative %39Ar Released